Biomedical & Pharmacology Journal, September 2024. Vol. **17**(3), p. 1769-1783

In-silico Investigation and Development of Cyclooxygenase-2 (1CX2) Selective Inhibition as a Possible Anti-Inflammatory Activity

Ramu Samineni[1], Prasanthi Samathoti[2], Sampath A. Gouru[3], Anwar Khan[4], Preethi Priyadharshni SP[5], Kiran Manda[6], Vijay Kishore M[7] and Naresh Podila[8]*

[1]Department of Pharmaceutics, School of Pharmacy, Joy University, Raja Nagar, Vadakangulam, Near Kanyakumari, Tirunelveli, Tamil Nadu, India.
[2]Department of Pharmaceutics, MB school of Pharmaceutical Sciences, Mohan Babu University, Sree Sainath Nagar, Rangampet, Tirupati, Andhra Pradesh, India.
[3]Department of Quality Assurance, EQRX International Inc. Cambridge, Massachusetts, USA.
[4]Department of Pharmaceutics, ERA College of Pharmacy, ERA university, Sarfaraz Ganj, Lucknow, U. P., India.
[5]Department of Pharmacognosy and Phytochemistry, School of Pharmacy, Haramaya University. Rd, Harar, Ethiopia.
[6]Shri Vishnu College of Pharmacy, Garagaparru Road, Kovvada, Bhimavaram, Andhra Pradesh, India.
[7]Department of Pharmaceutical Chemistry, Acharya Nagarjuna University, Guntur, Andhra Pradesh, India.
[8]School of Biotechnology and Pharmaceutical Sciences, Vignan's Foundation for Science, Technology and Research, Guntur. Andhra Pradesh, India.
*Corresponding Author E-mail: nareshtrcp10@gmail.com

https://dx.doi.org/10.13005/bpj/2982

(Received: 13 April 2024; accepted: 26 July 2024)

Nonsteroidal anti-inflammatory drugs (NSAIDs) that specifically target the enzyme cyclooxygenase-2, or COX-2, which causes inflammation and discomfort, are known as COX-2 inhibitors. The objective of this work is to perform the anti-inflammatory activity, and molecular docking studies of compounds. We aim to develop new drug phytochemicals as anti-inflammatory agents targeting COX-2(PDB ID: 1CX2) for treatment. To find potential molecules, the PyRx 0.8 tool has been used to dock 37 potent molecules against COX-2 (PDB ID: 1CX2). The top scorer molecules (phytochemicals) (Dihydromyricetin, Catechin, Chlorogenic acid, Chrysin, and Emodin) were selected. Prior to further analysis, the compounds underwent thorough in vivo evaluation to assess their toxicity and anti-inflammatory properties. The results indicated that dihydromyricetin, catechin, and chlorogenic acid were the sole substances that exhibited both negligible acute toxicity and superior anti-inflammatory properties, surpassing the efficacy of diclofenac sodium, the established medicine. Among the compounds that were evaluated, Dihydromyricetin was shown to possess the most powerful anti-inflammatory properties due to its trihydroxy phenyl chroman-4-one substitution. Correlated to diclofenac (-8.5 Kcal/mol), dihydromyricetin and catechin showed significant bounden affinity, with the lowest binding free energies (-9.9 and -9.2 Kcal/mol) according to the computational study. This correlation between in silico and in vivo studies validated these compound's powerful anti-inflammatory properties.

Keywords: Anti-inflammatory; COX-2; Molecular docking studies; Potent phytochemicals.

This is an Open Access article licensed under a Creative Commons license: Attribution 4.0 International (CC-BY).
Published by Oriental Scientific Publishing Company © 2024

An enzyme called cyclooxygenase (COX) aids in the production of prostaglandins. The body naturally produces prostaglandins, which are essential for inducing inflammation. An increased number of prostaglandins is found in the body's inflammatory regions[1]. characterized by visible and palpable signs of swelling, redness, and discomfort. Arachidonic acid (AA) is the precursor to prostaglandins. In the body, as fatty acids and amino acids are distinct types of molecules. The building blocks of lipids are called fatty acids, which are essential to bodily function. The enzyme that converts AA into prostaglandins is COX. Arachidonic acid is transformed into thromboxane A2 (TxA2) by COX. Platelets are activated by a signal from TxA2 to initiate clot formation. Additionally, it constricts blood vessels, acting as a vasoconstrictor[2].

COX Pathway

Prostaglandin G/H synthases (PGHS), the enzymes responsible for metabolizing AA into PGH2 and PHG2, are commonly referred to as COX. Several subsequent enzymes utilize these prostaglandins, such as PGD2, PGE2, PGF2, PGI2, and TXA2, as their substrates[3]. The primary distinction between the two COX enzymes lies in the fact that COX-2 is an enzyme that is produced in response to certain stimuli, with a few noteworthy exceptions, whereas COX-1 is an enzyme that is consistently and widely expressed. The cytosolic PGE synthase (PGES) isozymes, PGF synthase, and thromboxane synthase are the most favoured, although not the only, partners of COX-1. These findings indicate that there is a specific and targeted interaction between COX and downstream synthases[4]. However, COX-2 is more inclined to provide PGH2/G2 to the isozymes of microsomal (m) PGES and prostaglandin I synthase (PGIS), which are frequently stimulated together by cytokines and tumor promoters[5].

The prostanoid receptor subfamily consists of five receptors: the PGD receptor (DP1), PGF receptor (FP), PGI receptor (IP), thromboxane receptor (TP), and four subtypes of the E prostanoid receptor, which has a total of eight members. PGs work by stimulating G protein-coupled receptors that are located on the membrane. Alternative splicing contributes to the complexity of the issue by resulting in eight distinct copies of EP3 with only their C-terminal tails and two additional isoforms of the human FP (FPA, FPB) and TP (TPá, TPâ) receptors[6]. Additionally, PGD2 has the ability to activate chemo attractant receptor-homologous molecule (CRTH2 or DP2), a unique G protein-coupled receptor that is part of the chemokine receptor family and is expressed on cells of T helper 2. The effects of prostanoid receptor activation on cell function are mediated by a frequence of intracellular signalling pathways. On the other hand, the activation of FP and EP1 receptors links to the metabolism of phosphatidylinositol through Gq, which causes the intracellular free calcium to be mobilised and inositol trisphosphate to be produced. To increase intracellular cAMP, for example, adenylyl cyclase is activated via Gs by the EP2, EP4, IP, and DP1 receptors[7].

Prostanoids like thromboxane, prostacyclin, and prostaglandins are synthesised with the help of COX. Arachidonic acid is converted by COX to prostaglandin H2 (PGH2), which is the first and rate-limiting step in the synthesis of prostanoid. The drugs which are showing high potent activity will go and act upon cyclooxygenase and inhibits the production of prostaglandins, prostacyclin, and thromboxane[8-10]. Our drugs like Silybilin, Dihydromyrecitin and Gmelinol may have the property to suppress the cyclooxygenase (COX) enzyme[11-14].

MATERIALS AND METHODS

***In-silico* study**

The selected ligand structures are downloaded for PubChem in 3D (SDF Format). By using an online SMILES translator (https://cactus.nci.nih.gov/translate/) the molecules are converted from SDF format to PDB format. The selected Protein (COX-2) is prepared by using Discovery Studio Visualizer software. The protein has been uploaded in DS Visualizer by selecting the file option. After the unwanted chains, hetero atoms, and water molecules are removed from the protein[15]. After removing check, the missing Amino Acids and fill the gaps from the PDB, and add polar Hydrogen.

Docking study

A docking study of a few chosen phytochemicals against the COX-2 protein (PDB ID: 1CX2) was conducted using PyRx 0.8. PyRx is a Python programming language that can be

used on nearly any modern device, including supercomputers and desktop computers. PyRx has been used to help with molecular docking by determining a ligand's binding affinity for a protein. With a resolution of 3.00 Å, all 22 phytochemicals were screened for COX-2 (PDB: 1CX2) using PyRx, a structure-based docking program. Following the docking evaluation, in PyRx software the protein is uploaded, converted into macromolecule and ligands are also uploaded, ligands energy is minimized, and they are converted into PDBQT format. A molecular window including all of the designated active sites is used for molecular docking. The PyRx scores were used to categorize ligands based on their binding affinities. The ligands were then categorized based on the degrees of binding energy they possessed[16, 17].

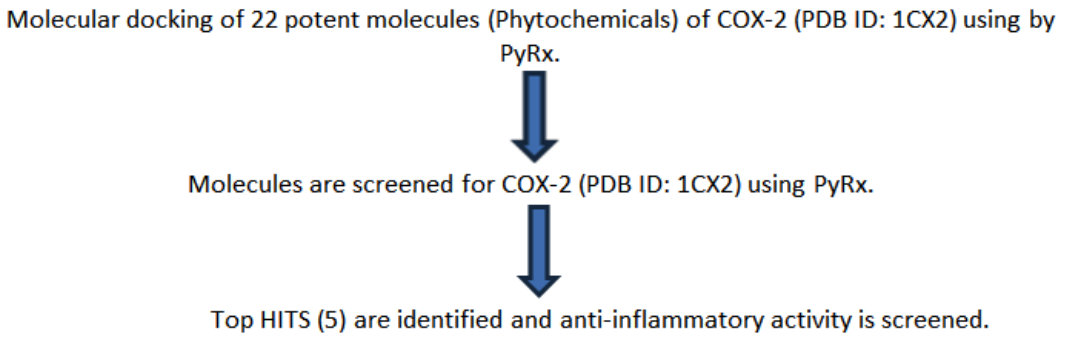

Chart 1. Docking study

Rule of 5 (Lipinski's rule)

Comparable drugs, drug-likeness assesses a molecule's bioavailability to determine its suitability as an oral drug. Its crimson, twisted hexagon within the pink color is what makes it unique. Swiss ADME uses five different rule-based filters that are sourced from large pharmaceutical companies to filter chemical libraries to remove molecules with characteristics that are incompatible with a suitable pharmacokinetics profile. This process improves the state of proprietary chemical collections[18]. Five rules are available for describing small compounds using the Lipinski filter (Pfizer) based on their physicochemical property profiles: Lower than 500 molecular weight (MW), MLOGP d" 4.15, 10 N or O, and NH or OH < 5. According to Lipinski, all nitrogen's and oxygen's with at least one hydrogen atom are H-bond donors, while all other nitrogen's and oxygen's are H-bond acceptors. Furthermore, Lipinski et al. state that aliphatic fluorines are acceptors while alanine nitrogens are neither donors nor acceptors[19].

Small compounds with physicochemical properties, functional groups, and substructures are described by the Ghose filter (Amgen). A tiny molecule with 20–70 atoms meets the qualifying range[20]. In addition, to be eligible, the total number of atoms' molar refractivity (MR) must be between 40 and 120, the molecular weight must be between 160 and 484 Da, and the WlogP must be between -0.5 and 5.4. A molecule is considered drug-like if it has twelve or fewer H-bond donors and acceptors, ten or fewer rotatable bonds, and a TPSA of 140 Å2, as per the Veber filter (GSK filter) model. Strong oral bioavailability is expected for these drugs, and increased rotatable bond numbers hurt penetration rate; decreasing TPSA is correlated with increased penetration rate[21]. The Egan filter (Pharmacia filter), which is reliant on the principles underpinning a small molecule's membrane permeability, predicts drug absorption. For instance, if a molecule's TPSA is less than 134.2 and its WLOGP is less than 5.68, this model describes it as a pharmaceutical. The human passive intestinal absorption (HIA) of tiny substances using the Egan computer model is a reliable tool for predicting drug absorption since it accounts for both efflux and active transport channels[22].

Drug-like and non-drug-like molecules are separated by the Muegge filter, also known as the Bailey filter. It is an independent Pharmacophore point filter. A molecule is represented as a drug in

this model if its molecular weight is between 200 and 610 Da, its Total polar surface area is 150, its XLOGP is between -2 and 5, etc. As per reference[23], The following characteristics are applicable: The quantity of rings is fewer than seven, the quantity of carbon atoms is greater than four, the quantity of heteroatoms is greater than one, the quantity of rotatable bonds is less than fifteen, the quantity of H-bond acceptors is less than ten, and the quantity of H-bond donors is less than five. The Abbott bioavailability value aims to estimate the likelihood of a chemical having at least 10% oral bioavailability in rats by assessing the permeability of Caco-2, which envisions the chance of a chemical having F>10% based on the predominant charge at physiologic pH in a rat model. Its primary objective is to swiftly filter chemical libraries to find the most suitable chemicals for synthesis[24].

***In-vivo* studies**

Acute oral toxicity

According to the OECD 423 recommendations, we used the acute toxic class technique to assess the target compounds' toxicity in the current experiment. In this study, Swiss albino rats weighing 200–250 grams were employed. To evaluate the toxicity of the synthesized compounds, each group consisted of three rats of the same gender. A initial dose of 200 mg/kg body weight was given. Before receiving any medication, female rats were fasted for three to four hours without food or water. The animals' weights were determined after the fasting period, and 200 mg/kg of body weight of the synthesized derivatives were given orally[25]. Following the delivery of the test chemical, the animals were closely monitored for the first four hours at 30-minute intervals, and then every hour for up to twenty-four hours. Throughout the course of the 14-day observation period, every animal was carefully examined to look for any unexpected changes in its behavioural, biological circumstances[26].

Carrageenan–Induced Rat Paw Edema Model

The study that we conducted with the carrageenan-induced paw edema[27] included male and female healthy rats weighing between 100 and 190 grams. Three sets of six test animals each were created out of these rats. The animals fasted for the whole night before the trial started, with access to water given as needed[28]. A normal saline solution was given to the control group (negative control), while 20 mg/kg of dihydromyricetin was given to the second group, Catechin was given to the third group, Chlorogenic acid was given to the fourth group, and 4.5 mg/kg of the standard medication, diclofenac sodium, was given to the fifth group. Using an oral catheter, each test and standard material was given orally after being dissolved in normal saline[29]. An injection of a 0.2 ml solution containing 1% w/v carrageenan was administered into the subplantar area of the rats' right paw in order to induce edema. Once the paw was marked with ink up to the level of the lateral malleolus, it was then submerged in mercury up to the specified point. Subsequently, a Plethysmometer was employed to quantify the extent of edema in the rat's paw[30,31]. After injecting carrageenan, the paw volumes of each group were measured immediately (at 0 hours) and then every hour for the next two hours. The precise quantification of the paw size growth was determined by subtracting the beginning data from the end values. The rats who received medication were compared to a group of rats that did not get any treatment in order to calculate the average increase in the size of their paws. Subsequently, a formula was employed to calculate the proportion that prevented the occurrence of edema[32].

$$\% \text{ inhibition} = \frac{1 - Vt}{Vc} \times 100$$

Were,

Edema volume is represented by "Vc" in the control

"Vt" represents the amount of fluid accumulation in the group that received the experimental medicine. The values are the average plus or minus the standard error of the mean (SEM) of six animals in each group.; $p<0.001$% inhibition indicates statistically significant differences from the control. Tuckey's test was run after an ANOVA was used for statistical analysis.

RESULTS AND DISCUSSION

***In-silico* studies**

The protein data bank provided the three-dimensional structure of cyclooxygenase-2 (PDB: 1CX2). The protein-ligand interaction profile (PLIP) was used to determine the active site amino acid residues. As seen in Figure 1, the amino acid

residues that are present in the catalytic pocket are GLU A:67, ASN A:68, and TYR A:55. The Ramachandran plot, which is depicted in Figure 2, confirmed the prepared protein.

Docking study

To precisely predict the optimal shape of both drug candidates (as ligands) and their targets, receptor proteins, to form a stable complex, molecular docking studies have been carried out. The next phase involved searching for the binding site and binding pockets following the development and import of the protein receptor file from the Protein Data Bank. The ligands were guided through the molecular docking process by binding pockets. Table 1 displays the binding location and docking pose of the ligands interacting with residues of amino acids, and displays the hydrogen bonds created with the amino acids from group interaction atoms, the interacting group, and the docking score. Among all the molecules

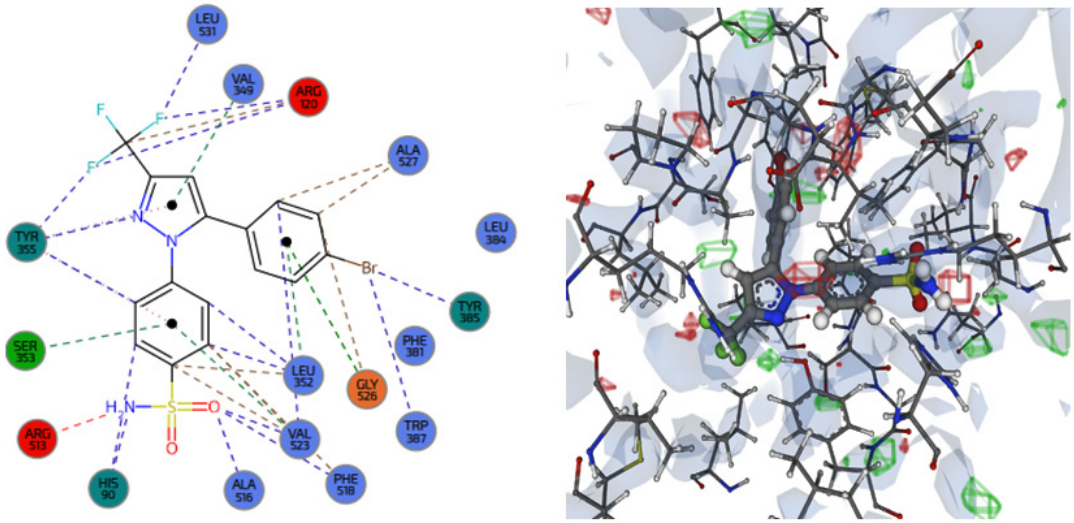

Fig. 1. Residues of amino acids found in the catalytic pocket's active site

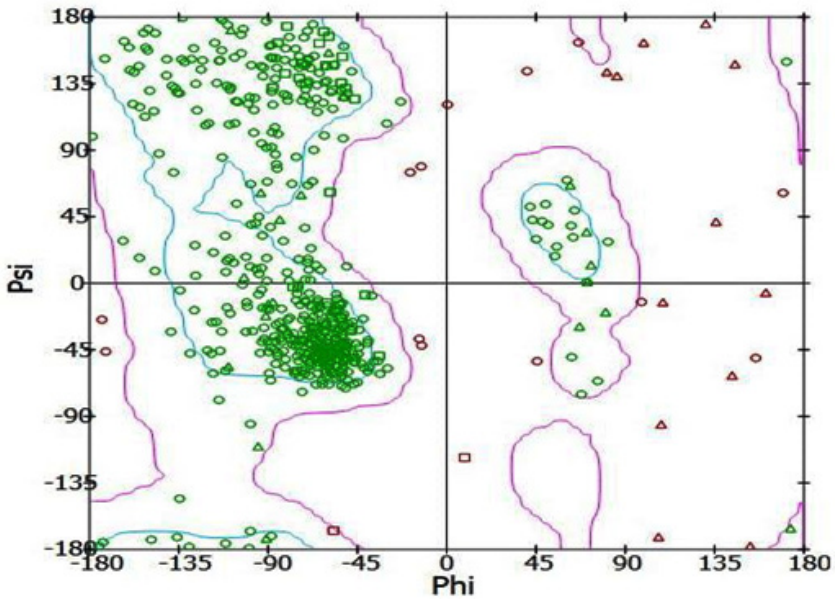

Fig. 2. Ramachandran plot of 1CX2

Table 1. Binding energies and amino acid interactions of selected compounds

S. No	Compound	Chemical Structure	Binding Energy (Kcal/mol)	No of Hydrogen bonds	Interacting amino acid residues
1	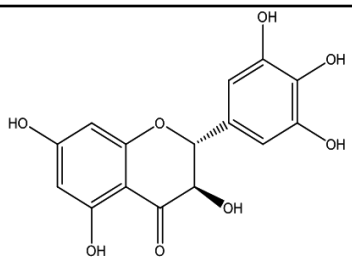 (2*R*,3*R*)-3,5,7-trihydroxy-2-(3,4,5-trihydroxyphenyl)chroman-4-one	Dihydro myricetin	-9.9	5	Cys 37, Cys 41, Cys 47, Gly 45, Arg44
2	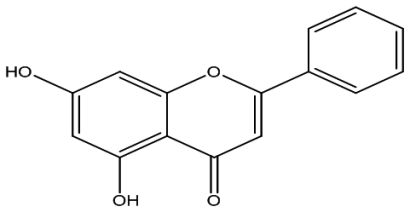 5,7-dihydroxy-2-phenyl-4*H*-chromen-4-one	Catechin	-9.2	3	Cys 36, Cys 47, Glu 465
3	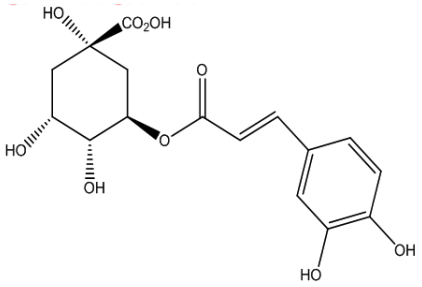 (1*S*,3*R*,4*R*,5*R*)-3-(((*E*)-3-(3,4-dihydroxyphenyl)acryloyl)oxy)-1,4,5-trihydroxycyclohexane-1-carboperoxoic acid	Chlorogenic Acid	-9.1	3	Arg 44, Gly 45, Pro 154
4	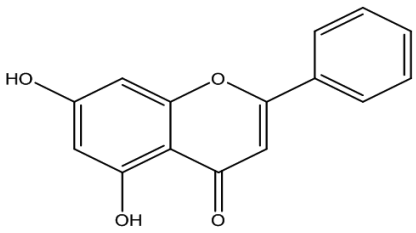 5,7-dihydroxy-2-phenyl-4*H*-chromen-4-one	Chrysin	-9.1	4	Cys 45, Gly 45, Glu 465, Gln 461
5	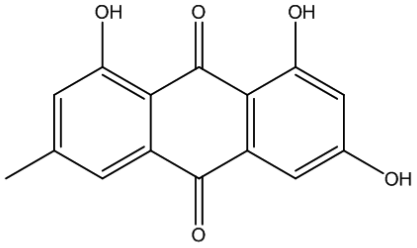 1,3,8-trihydroxy-6-methylanthracene-9,10-dione	Emodin	-9.0	4	

\					
6	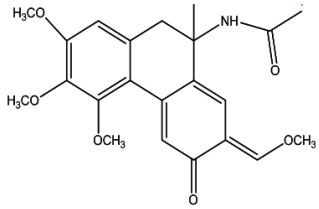 (*E*)-*N*-(2,3,4-trimethoxy-7-(methoxymethylene)-9-methyl-6-oxo-6,7,9,10-tetrahydrophenanthren-9-yl)acetamide	Colchine	-6.9	2	Tyr 254, Arg 307
7	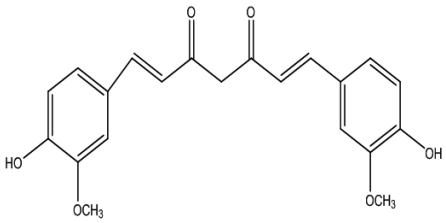 (1*E*,6*E*)-1,7-bis(4-hydroxy-3-methoxyphenyl)hepta-1,6-diene-3,5-dione	Curcuminoids	-8.7	1	Gln 289
8	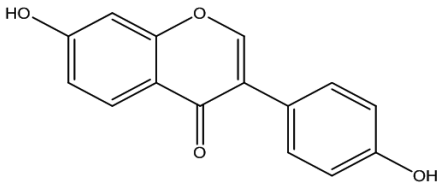 7-hydroxy-3-(4-hydroxyphenyl)-4*H*-chromen-4-one	Diadzein	-8.6	1	Gln 461
9	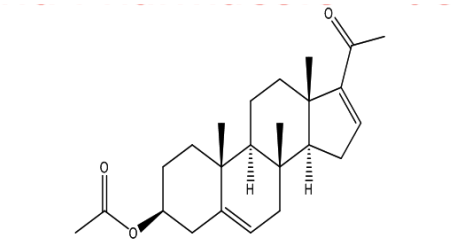 (3*S*,8*R*,9*S*,10*R*,13*S*,14*S*)-17-acetyl-8,10,13-trimethyl-2,3,4,7,8,9,10,11,12,13,14,15-dodecahydro-1*H*-cyclopenta[*a*]phenanthren-3-yl acetate	16 DPA	-8.1	2	Asn 34, Arg 44
10	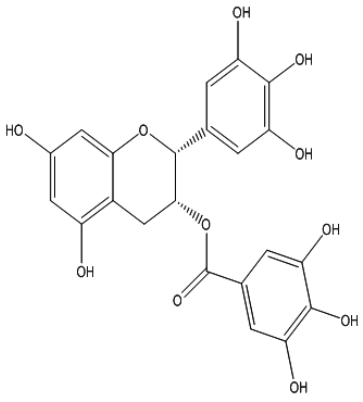 (2*R*,3*R*)-5,7-dihydroxy-2-(3,4,5-trihydroxyphenyl)chroman-3-yl 3,4,5-trihydroxybenzoate	Epigallocatechin Gallate (EGCG)	-8.7	4	Asp347, Glu346, Ser579, His356

11	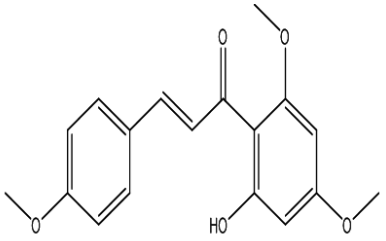 (*E*)-1-(2-hydroxy-4,6-dimethoxyphenyl)-3-(4-methoxyphenyl)prop-2-en-1-one	Flavokawin A	-8.5	1	Phe200
12	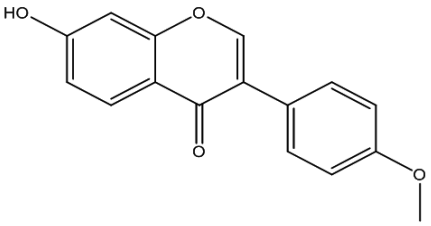 7-hydroxy-3-(4-methoxyphenyl)-4*H*-chromen-4-one	Formononetin	-8.6	1	Cys47
13	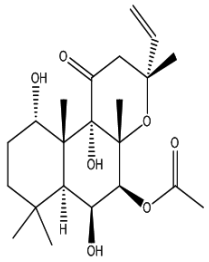 (3*R*,4a*R*,5*S*,6*S*,6a*S*,10*S*,10a*R*,10b*S*)-6,10,10b-trihydroxy-3,4a,7,7,10a-pentamethyl-1-oxo-3-vinyldodecahydro-1*H*-benzo[*f*]chromen-5-yl acetate	Forskolin	-7.0	2	Tyr122, Ser471
14	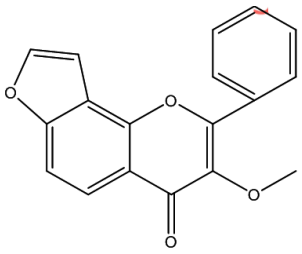 3-methoxy-2-phenyl-4*H*-furo[2,3-*h*]chromen-4-one	Karanjin	-8.0	1	His207
15	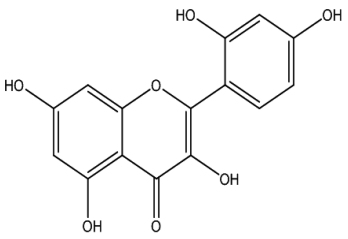 2-(2,4-dihydroxyphenyl)-3,5,7-trihydroxy-4*H*-chromen-4-one	Morin Hydrate	-8.3	3	Cys36, Gly45, Tyr130

16	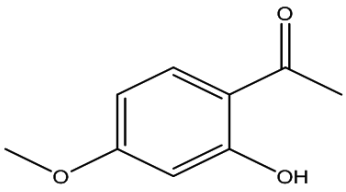 1-(2-hydroxy-4-methoxyphenyl)ethan-1-one	Paeonol	-6.6	2	Gln203, His207
17	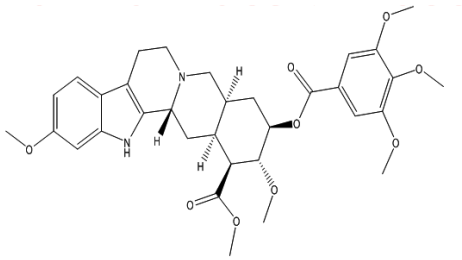 methyl (1*S*,2*R*,3*R*,4a*S*,13b*R*,14a*S*)-2,11-dimethoxy-3-((3,4,5-trimethoxybenzoyl)oxy)-1,2,3,4,4a,5,7,8,13,13b,14,14a-dodecahydroindolo[2',3':3,4]pyrido[1,2-*b*]isoquinoline-1-carboxylate	Reserpine	-8.7	1	His 214
18	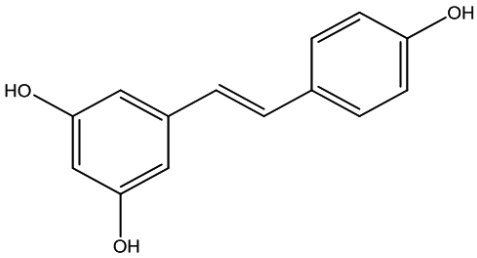 (*E*)-5-(4-hydroxystyryl)benzene-1,3-diol	Resveratrol	-7.8	2	Asn34, Glu 465
19	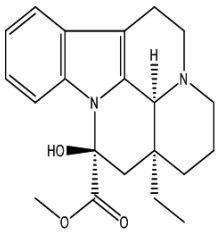 methyl (4^{1}*S*,12*S*,13a*S*)-13a-ethyl-12-hydroxy-2,3,4^{1},5,6,12,13,13a-octahydro-1*H*-indolo[3,2,1-*de*]pyrido[3,2,1-*ij*][1,5]naphthyridine-12-carboxylate	Vincamine	-7.5	1	His 214
20	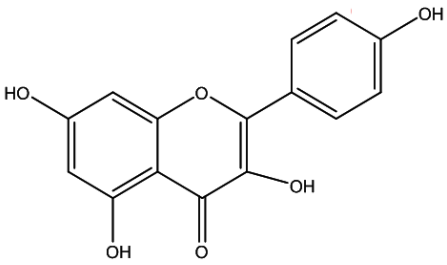 3,5,7-trihydroxy-2-(4-hydroxyphenyl)-4*H*-chromen-4-one	Kaempferol	-8.9	4	Cys37, Cys47, Ala 156, Gln 461

21	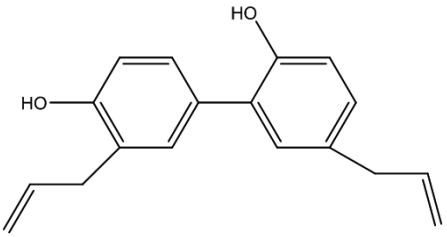 3',5-diallyl-[1,1'-biphenyl]-2,4'-diol	Honokiol	-8.9	4	Cys 47, Ala 156, Cys 159, Gln 461

Table 2. Selected Drugs and Their Molecular Properties

S No	Name of the compound	miLogP	TPSA	natms	MW	nviolations	nrotb
1	Dihydromyricetin	-1.16	147.68	23	320.25	1	8
2	Catechin	0.24	110.38	21	290.27	0	6
3	Chlorogenic acid	-1.05	164.75	25	354.31	1	9
4	Chrysin	1.08	70.67	19	254.24	0	4
5	Emodin	0.36	94.83	20	270.24	0	5
6	Colchine	0.79	83.09	29	399.44	0	6
7	Curcuminoids	1.47	93.06	27	368.38	0	6
	Diadzein	1.08	70.67	19	254.24	0	4
8	16 DPA	4.22	43.37	26	356.5	1	3
9	Epigallocatechin	-0.18	197.37	33	458.37	2	11
10	Flavokawin A	1.75	64.99	23	314.33	0	5
11	Formononetin	1.33	59.67	20	268.26	0	4
12	Forskolin	0.81	113.29	29	410.5	0	7
13	Karanjin	1.67	52.58	22	292.29	0	4
14	Morin Hydrate	-0.56	131.36	22	302.24	0	5
15	Paeonol	0.83	46.53	12	166.17	0	3
16	Reserpine	1.75	117.78	44	608.68	2	10
17	Resveratrol	2.26	60.69	17	228.24	0	3
18	Vincamine	2.62	54.7	26	354.44	0	4
19	Kaempferol	-0.03	111.13	21	286.24	0	6
20	Honokiol	3.78	40.46	20	266.33	0	2

Table 3. Impact of certain compounds on rat paw edema

S. No.	Name	Rat paw edema volume (mm)			
		0 min	30 min	60 min	120 min
1	Dihydromyricetin (20 mg/kg)	0.61±0.00	0.51±0.03	0.45±0.03	0.27±0.02*
2	Catechin (20 mg/kg)	0.88±0.01	0.75±0.01	0.48±0.05	0.37±0.03*
3	Chlorogenic acid (20 mg/kg)	0.49±0.01	0.46±0.05	0.40±0.01*	0.30±0.00*
4	Diclofenac (20 mg/kg)	0.51±0.01	0.41±0.01	0.35±0.01*	0.24±0.02*
5	Control	0.31±0.04	0.38±0.02	0.26±0.02	0.35±0.01

Values are provided as mean ± SEM, *p<0.05, and are assessed using one-way ANOVA and Tukey's multiple comparison test. There are six values in all.

some are showing more binding energies with the COX-2 receptor within the active site and the interactions are Catechin has interactions with the Amino acids (ARG:44, CYS:47, CYS:36, PRO:153, LEU:152, GLU:465, ARG:469),Chrysin has interactions with the Amino acids (ALA:156, CYS:36, GLU:46, PRO:153, CYS:47, GLY:45, LEU:152, GLU:465, GLN:461), Dihydromyricetin has interactions with the Amino acids(CYS:47, ARG:44, GLY:45, CYS:41, PRO:153, CYS:36, CYS:37, VAL:155), Emodin has interactions with the Amino acids (GLU:465, GLN:461, PRO:153, ARG:469, CYS:47, GLU:46, LEU:152), Gmelinol has interactions with the Amino acids (ARG:44, GLU:465, PRO:153, CYS:47, CYS:36, LYS:468), Hecogenin exhibits interactions with the amino acids TYR:122 and LEU:80. Similarly, Juglone also interacts with the amino acids TYR:122 and LEU:80. On the other hand, Oleanolic acid interacts specifically with the amino acid TYR:122, Papaverin Hcl has interactions with the Amino acids (GLN:289, LEU:294, HEM:682, VAL:291, HIS:214), Silybilin has interactions with the Amino acids (CYS:41, ASN:39, PRO:153, CYS:36, ASN:34, PRO:154, ALA:156, ASP:157, TYR:136, GLY:135). We will conduct additional in-vitro tests on the compounds based on these results.

Rule of 5 (Lipinski's rule)

Swiss ADME was used to evaluate the physicochemical properties of the chosen drug candidates to determine their drug similarity. The results are reported in Table 2. All exhibit qualities similar to drugs, according to the results.

Acute Oral Toxicity Study

The oral acute toxicity study was conducted using the OECD guideline-423 methodology. This approach was created to examine substances at fixed dosages and offers data for both hazard assessment and the ranking of chemicals for hazard classification. By suspending the synthesized

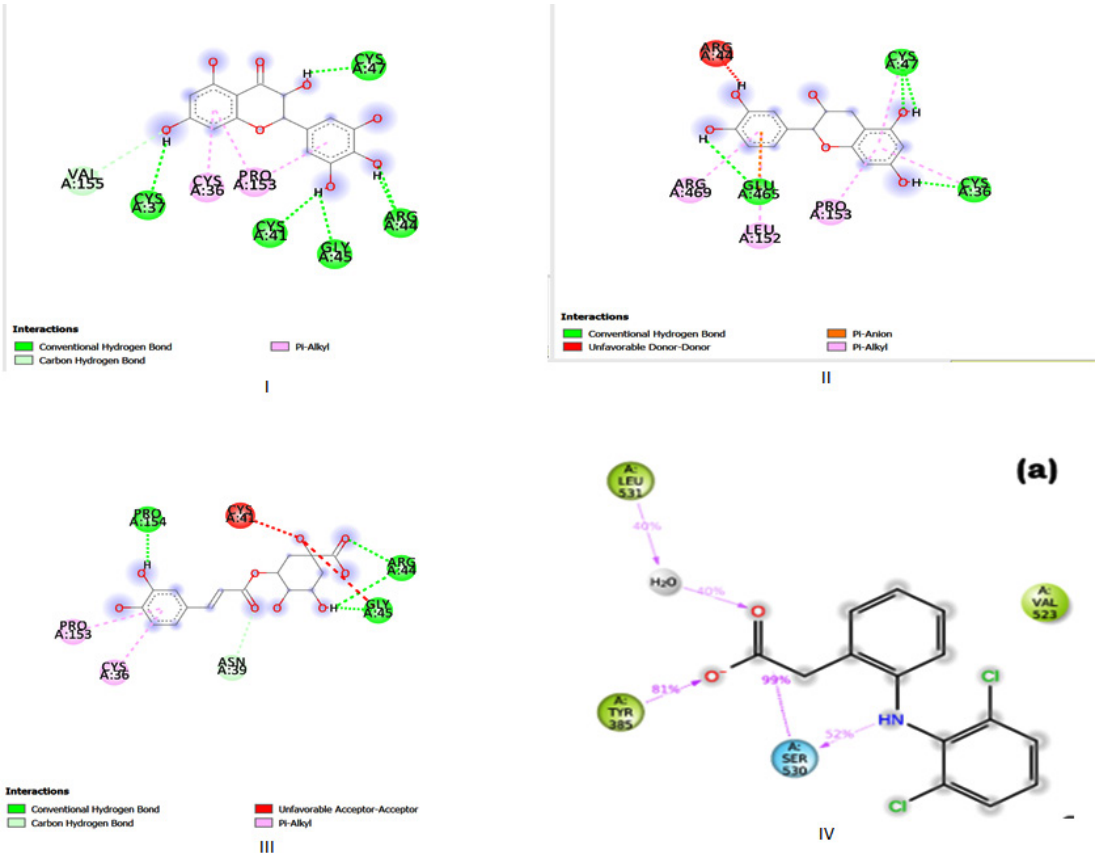

Fig. 3. Two-dimensional interactions between amino acid residues in proteins and their internal ligands, dihydromyricetin (I), catechin (II), chlorogenic acid (III), diclofenac (IV)

compounds in acacia and water, a starting dose of 200 mg/kg body weight was given, and the animals were monitored for 14 days after the administration sample. At least twice daily, careful observation was undertaken to look for any effects on the CNS, ANS, salivation, skin coloring, motor activity. The LD_{50} value of the synthesized ligands is indicated as class 5, as there was no evidence of toxicity at a dose of 200 mg/kg animals body weight. Of the five synthesized molecules, two derivatives (Chrysin and Emodin) were found as toxic, and the remaining three derivatives (Dihydromyricetin, Catechin, and Chlorogenic acid) were found as non-toxic at selected dose levels and well tolerated by the experimental animals as their LD_{50} cut of values were >200 mg/kg body weight, according to the data from the toxicity studies.

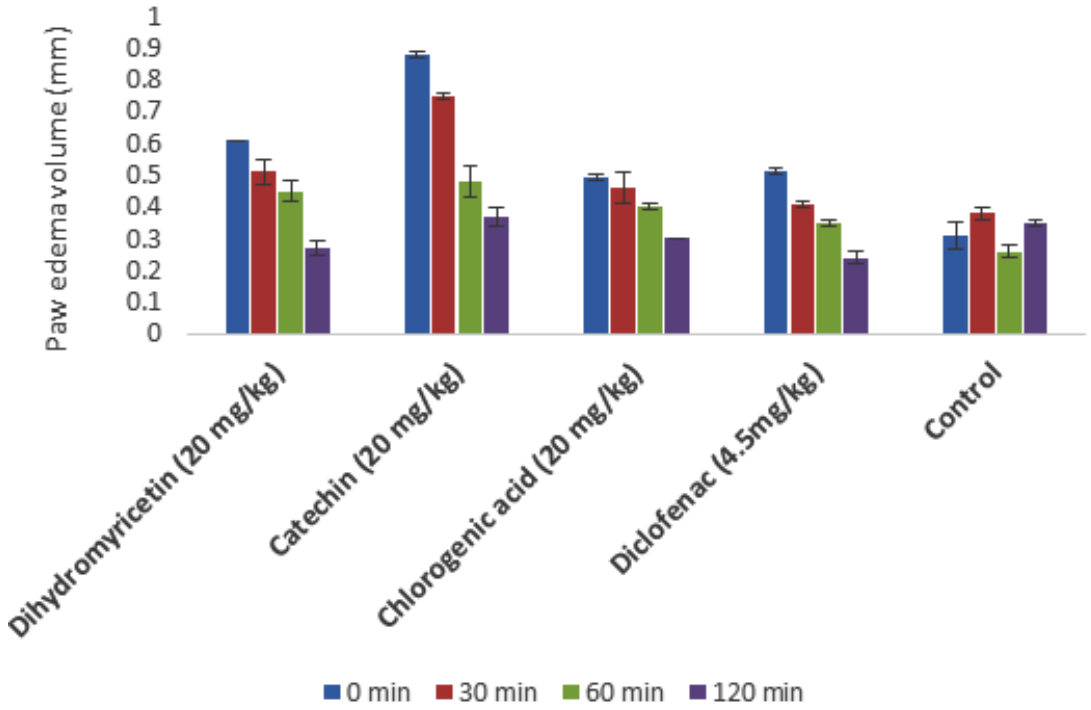

Fig. 4. Bar diagram with mean and standard error of the mean at 0-2 hrs

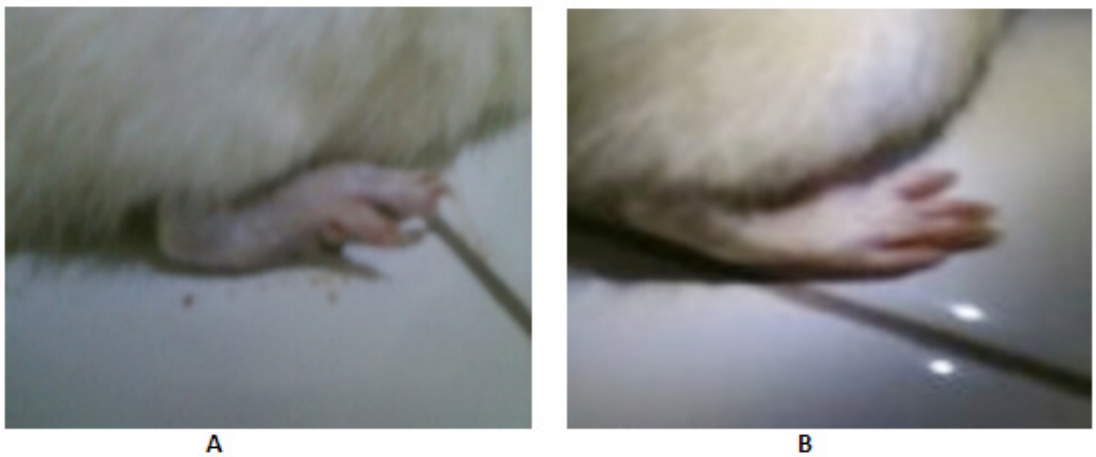

Fig. 5. Wistar rats with anti-inflammatory action.
A) Pre-treatment paw edema; B) Post-treatment paw edema

***In vivo* Rat Paw Edema Method**

We tested the anti-inflammatory activity of the synthesized molecules using rat paw edema (produced by carrageenan). The effects of the activity were timed at zero, thirty minutes, 1, and 2 hours, with dosages of 20 mg/kg of body weight being investigated. Table 3 presents the findings. The three compounds that were synthesized had varying degrees of anti-inflammatory properties. All three drugs show their maximal effects for up to two hours. The results obtained from the synthesized ligands, administered at a dosage of 20 mg/kg body weight, indicated that the most significant activity was observed when R was replaced with -CH3, phenyl, and phenyl carboxylate[57].

Figures 3 and 4 illustrate the comparative anti-inflammatory efficacy of synthetic derivatives (NTD1-NTD3) in relation to the reference drug diclofenac sodium. The data suggest that these three drugs exhibit significant (p 0.01) anti-inflammatory activity. The compounds exhibited the most significant impact at the 60 and 120-minute marks. This work shows how the target molecules inhibited prostaglandins, especially in the biphasic reaction that happened after carrageenan was administered. Furthermore, the cyclooxygenase enzyme may be selectively inhibited by these compounds. Figure 5 clearly demonstrates the disparity in paw edema volume between the test animals before and after treatment with the examined medications.

CONCLUSION

In-silico molecular docking simulations have been performed by inserting all of the selected medications into the preferred binding site of the protein receptor COX-2, using PyRx software to determine the orientation, binding affinities, and binding modes of all ligands. The docking experiments showed that every molecule had a good docking score. The results discussed in this study show that the selected phytochemicals show good activity. Among all the results top HIT molecules are selected for further in-vitro studies for anti-inflammatory activity. To sum up, these derivatives underwent a thorough assessment that included both computational and experimental methods in order to determine their potential as anti-inflammatory drugs. Notably, Chlorogenic acid, featuring a carboperoxoic acid and dihydroxy phenyl substitution, emerged as a promising lead compound, demonstrating remarkable anti-inflammatory properties in both in-silico and in vivo studies. Its binding affinity, stability, and interactions with the target protein COX-2 were found to be superior to the standard drug diclofenac sodium. Additionally, the safety profile of these derivatives was assessed, revealing that Dihydromyricetin, Catechin, and Chlorogenic acid exhibited no toxicity concerns at the tested dose levels, while Chrysin and Emodin displayed undesirable toxic effects. This highlights the need for careful consideration of toxicity in drug development. The findings from this research offer valuable insights into the potential of Chlorogenic acid as a lead compound for the buildout of anti-inflammatory drugs. However, further investigations are warranted to explore the structure-activity relationship and the precise mechanisms underlying the observed anti-inflammatory activity. Overall, this study highlights the latent of chlorogenic acid as a key option in the hunt for some more potent anti-inflammatory medicines and lays the groundwork for future research in the field of drug design and development.

ACKNOWLEDGEMENTS

The authors acknowledge the management of Vignan's Foundation for Science, Technology and Research, Vadlamudi, Guntur, for providing the opportunity to carry out this research work.

Conflicts of Interest

The author declare that there are no conflicts of interest.

Funding Sources

There is no funding Sources.

Author Contributions

Concept – N.P.; Design – N.P; Resource – N.P, P.S; Materials – P.P, K.M; Data Collection &/or Processing – S.A.G, P.S.; Analysis &/or Interpretation – N.P; Literature Search – N.P, A.K; Writing – N.P, R.S; Critical Reviews – N.P, K.M

REFERENCES

1. Naresh P and Choudhary, T. Synthesis of Some Dihydro pyrimidinone Derivatives and Study of Their Anti-Inflammatory Activity. Journal of

Applied Pharmaceutical Research., 2018; 6(1): 11-15.
2. Violette S. H and Ebtisam Abdel A.H. Synopsis of arachidonic acid metabolism: A review. Journal of Advanced Research., 2018; 11: 23-32.
3. Wang B, Wu L, Chen J, Dong L, Chen C and Wen, Z. Metabolism pathways of arachidonic acids: mechanisms and potential therapeutic targets. Signal Transduct Target Ther., 2021; 6(1): 94.
4. Jang Y, Kim M and Hwang S. W. Molecular mechanisms underlying the actions of arachidonic acid-derived prostaglandins on peripheral nociception. J Neuroinflammation., 2020; 17: 30.
5. de Souza do Nascimento J, Carlos R, Delgado-Azanero W, Mosqueda Taylor A, de Almeida O. P, Romanach M. J and de Andrade B. A. Immunohistochemical expression of cyclooxygenase-2 (COX-2) in oral nevi and melanoma. J Oral Pathol Med. 2016; 45(6): 440-3.
6. Braune S, Küpper J. H and Jung F. Effect of Prostanoids on Human Platelet Function: An Overview. *International Journal of Molecular Sciences.,* 2020; 21(23): 9020.
7. Athari S. S. Targeting cell signaling in allergic asthma. Sig Transduct Target Ther., 2019; 4: 45.
8. Edward A, Dennis and Paul C, Norris. Eicosanoid storm in infection and inflammation. Nature Reviews Immunology., 2015.
9. Fujimori, K. Prostaglandin D_2 and $F_{2â}$ as regulators of adipogenesis and obesity. Biol. Pharm. Bull., 2022; 45:985-991.
10. Fujino H. The biased activities of prostanoids and their receptors: review and beyond. Biol. Pharm. Bull., 2022; 45:684-690 (2022).
11. Hajeyah A. A, Griffiths W. J, Wang Y, Finch A. J. and O'Donnell, V.B. The biosynthesis of enzymatically oxidized lipids. Front. Endocrinol*,* 2020; 11:591819.
12. Idborg H. and Pawelzik S. C. Prostanoid metabolites as biomarkers in human disease. *Metabolites,* 2017; 12:721.
13. Jin K. P, Qian C, Lin J. T. and Liu B. Cyclooxygenase-2-prostaglandin E2 pathway: A key player in tumor-associated immune cells. Front. Oncol*.,* 2023; 13:1099811.
14. Kim, Y. and Stanley, D. Eicosanoid signaling in insect immunology: new genes and unresolved issues. Genes, 2021; 12:211.
15. Naresh P, Swaroop A. K, Esakki Muthu Kumar M, Shyam Sundar P, Amarnath G. S, Thirumoorthy A, Dharmaraja S and Jubie S. Identification of plant secondary metabolites as dengue envelope protein entry inhibitors through an in-silico approach. Journal of medical pharmaceutical and allied sciences., 2022; 11(4): 5085-5095.
16. Naresh P, Mithun R, Subramanyam S, Atul RB Yanadaiah P, Molakpogu RB, Kiran M, Renzon Daniel C. P and Sreelatha M. *In-vitro* antimitotic activity and *in-silico* study of some 6-fluoro-triazolo-benzothiazole analogues. Pharmacia., 2023; 70(4): 887-894.
17. Naresh Podila, Naveen Kumar Penddinti, Mithun Rudrapal, Gourav Rakshit, Sathish Kumar Konidala, Veera Shakar Pulusu, Richie R. Bhandare, Afzal B. Shaik. Design, synthesis, biological and computational screening of novel pyridine-based thiadiazole derivatives as prospective anti-inflammatory agents. Heliyon10(2024) e29390.
18. Naresh P, Shyam Sunder P and Jubie S. Dengue Virus Entry/Fusion Inhibition by Small Bioactive Molecules: A Critical Review. Mini-Reviews in Medicinal Chemistry., 2022; 22 (3); 484 – 497.
19. Lipinski C. A, Lombardo F, Dominy B. W and Feeney P. J. Experimental and computational approaches to estimate solubility and permeability in drug discovery and development settings. Adv Drug Deliv Rev., 1997; 23 (4).
20. Mahanthesh M. T, Ranjith D, Raghavendra Y, Jyothi R, Narappa G and Ravi M. V. Swiss ADME prediction of phytochemicals present in Butea monosperma (Lam.) Taub. Journal of Pharmacognosy and Phytochemistry., 2020; 9(3): 1799-1809.
21. Veber D. F, Johnson S. R, Cheng H. Y, Smith B. R, Ward K. W and Kopple K. D. Molecular properties that influence the oral bioavailability of drug candidates. J. Med. Chem., 2002; 45: 2615–2623.
22. Bojarska J, Remko M, Breza M, Madura I. D, Kaczmarek K, Zabrocki J and Wolf W. M. A Supramolecular Approach to Structure-Based Design with A Focus on Synthons Hierarchy in Ornithine-Derived Ligands: Review, Synthesis, Experimental and in Silico Studies. *Molecules.,* 2020;25(5):1135.
23. Muegge I, Heald S. L, Brittelli D. Simple selection criteria for drug-like chemical matter. J Med Chem., 2001, 7;44(12): 1841-6.
24. Alam S and Khan F. 3D-QSAR, Docking, ADME/Tox studies on Flavone analogs reveal anticancer activity through Tankyrase inhibition. Sci Rep., 2019, 1;9(1): 5414.
25. Deepti Shrimali, Muthu K. Shanmugam, Alan Prem Kumar, Jingwen Zhang, Benny K.H. Tan, Kwang Seok Ahn and Gautam Sethi. Targeted abrogation of diverse signal transduction cascades by emodin for the treatment of inflammatory disorders and cancer. Cancer Letters., 2013; 341 2(19): 139-149.

26. Smith D, Anderson D and Degryse A. D. Classification and reporting of severity experienced by animals used in scientific procedures: FELASA/ECLAM/ESLAV Working Group report. Laboratory Animals., 2018; 52(1) :5-57.
27. Rahman S and Jahan N. Anti-inflammatory activity of crude and detoxified leaves of Daphne oleoides Schreb. on carrageenan-induced paw edema in wistar rats. J Ayurveda Integr Med. 2021; 12(3): 500-505.
28. Ma J, Cheng Y, Su Q, Ai W, Gong L, Wang Y, Li L, Ma Z, Pan Q, Qiao Z and Chen K. Effects of intermittent fasting on liver physiology and metabolism in mice. Exp Ther Med., 2021 ;22 (3): 950.
29. Cong H. H, Khaziakhmetova V. N and Zigashina L. E. Rat paw oedema modeling and NSAIDs: Timing of effects. Int J Risk Saf Med., 2015; 27:76-7.
30. Minaiyan M. The anti-inflammatory effects of venlafaxine in the rat model of carrageenan-induced paw edema. Iranian Journal of Basic Medical Sciences., 2015; 18 (7):654-658.
31. Hossein Sadeghi, Valiolla Hajhashemi C, Mohsen Minaiyan C, Ahmad Movahedian D and Ardeshir Talebi. A study on the mechanisms involving the anti-inflammatory effect of amitriptyline in carrageenan-induced paw edema in rats. European Journal of Pharmacology., 2011; 667 (1): 396-401.
32. Semis H. S, Gur C, Ileriturk M, Kaynar O and Kandemir F. M. Investigation of the anti-inflammatory effects of caffeic acid phenethyl ester in a model of ë-Carrageenan–induced paw edema in rats. Human & Experimental Toxicology., 2021; 40(12): 721-738.